The Astrophysical Journal, 670:600–609, 2007 November 20

THE SPECTRAL ENERGY DISTRIBUTION OF QUIESCENT BLACK HOLE X-RAY BINARIES: NEW CONSTRAINTS FROM *SPITZER*

Elena Gallo,[1,2] Simone Migliari,[3] Sera Markoff,[4] John A. Tomsick,[5] Charles D. Bailyn,[6] Stefano Berta,[3,7] Rob Fender,[8] and James C. A. Miller-Jones[4]

Received 2007 May 2; accepted 2007 June 29

ABSTRACT

Among the various issues that remain open in the field of accretion onto black hole X-ray binaries (BHBs) is the question of how gas accretes at very low Eddington ratios, in the so-called quiescent regime. While there is general agreement that X-rays are produced by a population of high-energy electrons near the BH, there is controversy concerning the modeling of the contributions of inflowing versus outflowing particles and their relative energy budget. Recent *Spitzer* observations of three quiescent BHBs have shown evidence for excess emission with respect to the Rayleigh-Jeans tail of the companion star between 8–24 μm. We suggest that synchrotron emission from a partially self-absorbed outflow might be responsible for the observed mid-IR excess, in place of, or in addition to, thermal emission from circumbinary material. If so, then the jet synchrotron luminosity, integrated from radio to near-IR frequencies, exceeds the measured 2–10 keV luminosity by a factor of a few in these systems. In turn, the mechanical power stored in the jet exceeds the bolometric X-ray luminosity by at least 4 orders of magnitude. We compile the broadband spectral energy distribution (SED) of A0620−00, the lowest Eddington-ratio stellar mass BH with a known radio counterpart, by means of simultaneous radio, optical, and X-ray observations, and the archival *Spitzer* data. We are able to fit the SED of A0620−00 with a maximally jet-dominated model, in which the radio through the soft X-rays are dominated by synchrotron emission, while the hard X-rays are dominated by inverse Compton at the jet base. The fitted parameters land in a range of values reminiscent of the Galactic center supermassive black hole Sgr A*. Most notably, the inferred ratio of the jet acceleration rate to local cooling rates is 2 orders of magnitude weaker than higher luminosity, hard-state sources.

Subject headings: radiation mechanisms: general — stars: individual (A0620−00, V404 Cyg, XTE J1118+480) — X-rays: binaries

Online material: color figures

1. INTRODUCTION

The *Spitzer Space Telescope* offers for the first time the opportunity to identify and characterize the properties of highly sub-Eddington Galactic black hole X-ray binaries (BHBs) in the mid-infrared band, a frequency window that is still largely unexplored for these systems, and that may prove crucial to our understanding of the overall structure of the accretion flow in quiescence. The infrared (IR) spectra of BHBs with a low-mass donor star are likely shaped by a number of competing emission mechanisms, among which are the reprocessing of accretion-powered X-ray and ultraviolet photons, either by the donor star surface or by the outer accretion disk, direct thermal emission from the outer disk, nonthermal synchrotron emission from a relativistic outflow, and thermal emission from circumbinary dust. We refer the reader to Russell et al. (2006, hereafter R06), and references therein, for a recent comprehensive work on the optical and near-IR spectral properties of X-ray binaries. Here we wish to stress that, as well as for other wave bands, the relative strength of each mechanism is known to vary greatly in response to changes in the X-ray state of the system (see McClintock & Remillard 2006; Homan & Belloni 2005). Throughout this work, we shall focus on the IR properties of hard and quiescent low-mass BHBs. Such (generally transient) systems are characterized by strong variability, power-law-dominated X-ray spectra, and integrated X-ray luminosities that are largely sub-Eddington (roughly between a few $\times 10^{-6}$–10^{-2} times the Eddington luminosity, $L_{\rm Edd}$, for the hard state, and below a few $\times 10^{-6} L_{\rm Edd}$ for the quiescent state).

In spite of the large degree of uncertainty concerning the overall geometry of the accretion flow in this regime, there is general agreement that the X-rays are produced by a population of high-energy electrons close to the BH, and that the accreting gas is highly inefficient at radiating, as a result of either an intrinsically reduced radiative efficiency (Narayan & Yi 1994), a substantial mass loss (Blandford & Begelman 1999), or a combination of the two (e.g., Markoff et al. 2001; Yuan et al. 2005). The hard state is associated with the production of persistent, partially self-absorbed, synchrotron-emitting outflows with flat/inverted radio/millimeter spectra (Fender 2001). Such jets appear to survive down to quiescent X-ray luminosities (Gallo et al. 2006), even though sensitivity limitations on current radio telescopes make it extremely difficult to reach the signal-to-noise ratios (S/Ns) required to assess their presence for low-luminosity systems farther than 2 kpc or so. There is evidence from large-scale structures that the jets' mechanical power is comparable to the bolometric X-ray luminosity in some hard-state sources (e.g., Cyg X-1; Gallo et al.

[1] Physics Department, Broida Hall, University of California, Santa Barbara, CA 93106.
[2] Chandra Fellow.
[3] Center for Astrophysics and Space Sciences, 9500 Gilman Drive, University of California, San Diego, La Jolla, CA 92093.
[4] Astronomical Institute "Anton Pannekoek," University of Amsterdam, Kruislaan 403, 1098 SJ, Amsterdam, Netherlands.
[5] Space Sciences Laboratory, 7 Gauss Way, University of California, Berkeley, CA 94720.
[6] Department of Astronomy, Yale University, P.O. Box 208101, New Haven, CT 06520.
[7] Dipartimento di Astronomia, Università di Padova, Vicolo dell' Osservatorio 2, 35122 Padova, Italy.
[8] School of Physics and Astronomy, University of Southampton, Southampton SO17 1BJ, UK.

2005a; Russell et al. 2007). However, even for the highest quality spectral energy distribution (SED), disentangling the relative contributions of inflow versus outflow to the radiation spectrum and the global accretion energy budget can be quite challenging, as illustrated by the emblematic case of XTE J1118+480 in McClintock et al. (2003) and Markoff et al. (2001). Estimates of the total jet power based on its radiation spectrum depend crucially on the assumed frequency at which the flat, partially self-absorbed spectrum turns and becomes optically thin, as the jet radiative efficiency depends ultimately on the location of the high-energy cutoff induced by the higher synchrotron cooling rate of the most energetic particles. Once again, this quantity has proved hard to measure.

R06 have collected all the available quasi-simultaneous optical and near-IR data of a large sample of Galactic X-ray binaries over different X-ray states. The optical/near-IR luminosity of hard/quiescent BHBs correlates to the X-ray luminosity to the power $\sim$0.6, which is consistent with the known radio/X-ray correlation slope down to $10^{-8}L_{\rm Edd}$ (Gallo et al. 2006, but see Gallo 2007 and Xue & Cui 2007). Combined with the fact that the near-IR emission is largely suppressed in the thermal-dominant state (R06, Fig. 4), this leads to the conclusion that, for the BHBs, the break to the optically thin portion would take place in the mid-IR (2–40 μm). Additional evidence for a synchrotron contribution to the IR band in hard-state BHBs comes from variability studies during outbursts (e.g., Hynes et al. 2006; Homan et al. 2005). Indeed, from a theoretical point of view, the *break frequency*, here defined as the frequency at which the partially self-absorbed jet becomes optically thin, is inversely proportional to the BH mass; as jet spectral breaks are often observed in the GHz/submillimeter regime in active nuclei, they are expected to occur in the IR/optical band for 10^5–10^7 times lighter objects (see discussion in e.g., Markoff et al. 2001, and references therein). We know, however, from observations of GX 339−4, the only BHB where the optically thin jet spectrum has perhaps been observed (Corbel & Fender 2002; Homan et al. 2005), that the exact break frequency can vary with the overall luminosity, possibly reflecting changes in the magnetic field energy density, particle density, and mass loading at the jet base (Nowak et al. 2005). Determining the location of the jet break as a function of the bolometric luminosity is important in assessing the synchrotron contribution to the hard X-ray band, and may even highlight substantial differences among different classes of objects. As an example, the fact that the optically thin jet IR emission in GX 339−4 connects smoothly with the hard X-ray power law has led to a challenge of the standard Comptonization scenario for the hard X-ray state of BHBs (Markoff et al. 2001). In fact, recent *Spitzer* observations of the ultracompact neutron star X-ray binary 4U 0614+091 (while in a hard state) revealed that the break frequency must take place in the far-IR in this system, effectively ruling out a synchrotron origin for the X-ray power law (Migliari et al. 2006).

In addition to the jet, *Spitzer* observations of quiescent BHBs should be sensitive to possible emission from circumbinary material. Circumbinary disks may be formed as a result of mass outflow from the accretion disk, and have been invoked as an efficient process for the removal of orbital angular momentum, as well as for gravitational radiation loss and/or magnetic braking (see Taam & Spruit 2001 in the context of cataclysmic variables). Alternatively, circumbinary material could be due to the presence of a postsupernova explosion fallback disk, as is argued in the case of the anomalous X-ray pulsar 4U 0142+61 (Wang et al. 2006). Muno & Mauerhan (2006, hereafter MM06) report on *Spitzer* observations of four nearby low-mass X-ray binaries: three BHBs, plus one neutron star system. Excess mid-IR emission, with respect to the Rayleigh-Jeans tail of the donor blackbody spectrum, is detected from two (possibly all three) BH systems; MM06 attribute this bump to circumbinary dust illuminated by the low-mass companion star. This would imply that the optically thick-to-thin jet break occurs in the millimeter regime, at much lower frequencies than, e.g., inferred by R06.

In this paper, we aim to reassess the relative contribution of the various emission components to the radio/IR/optical spectra of the BHBs A0620−00, V404 Cyg, and XTE J1118+480 while in the quiescent state. We first report on the re-analysis of *Spitzer* observations, focusing on the rms estimate in the 24 μm data sets (§ 2), then proceed by examining the SED of each source (§ 3). The origin of the detected mid-IR excess emission is discussed in § 4. We finally focus on the broadband SED of A0620−00, a highly sub-Eddington ($L_{\rm X}/L_{\rm Edd} \simeq 10^{-8}$) BHB for which we put together previously published radio/X-ray data, the *Spitzer* data, and new optical data, all taken in 2005. We discuss the results of fitting the whole SED by means of a maximally jet-dominated model in § 5. A summary is given is § 6.

2. *SPITZER* OBSERVATIONS

The BHBs A0620−00, V404 Cyg, and XTE J1118+480 were observed by *Spitzer* between 2004 October and 2005 May as part of a survey of nearby low-mass X-ray binaries (PI: M. Muno; program 3289). Photometry of the three targets was acquired using the Multiband Imaging Photometer for *Spitzer* (MIPS; Rieke et al. 2004) at 24 μm and the Infrared Array Camera (IRAC; Fazio et al. 2004) at 8 and 4.5 μm. The Basic Calibrated Data (BCD) were reprocessed and then mosaicked with the MOPEX software (Makovoz & Marleau 2005), which uses single, multiframe, and dual outlier rejection. As discussed by MM06, in the case of A0620−00, the MIPS image was affected by dark latent features from a previous observation. The artifacts were corrected by dividing each BCD frame by a normalized median frame (based on all BCDs, excluding the source). These corrected BCDs were then mosaicked using MOPEX. Unique IR counterparts, consistent with the radio positions, are significantly (>5 σ) detected at 4.5 and 8 μm for all the three sources. The MIPS 24 μm images of the targets are shown in Figure 1; V404 Cyg and A0620−00 are detected at the 2–2.5 σ level, while XTE J1118+480 is undetected.

For each counterpart, we constructed the observation-specific point-response function (PRF) with PRF_ESTIMATE, and extracted the source flux using both standard aperture photometry on the background-subtracted image and PRF-fitting (using APEX), taking care to mask foreground stars. Sky subtraction was carried out through the use of multiple 10″ sky apertures placed over an annulus around the source. Table 1 lists the fluxes as measured using both aperture photometry and PRF-fitting on the mosaic images (the measured fluxes were then corrected for interstellar extinction following the standard prescription for the frequency-variable absorption by Cardelli et al. [1989]). While the values obtained with the two methods are consistent within the errors, both with each other and with the values measured by MM06, we derive systematically larger (typically by a factor 3) rms noise levels for the MIPS 24 μm fluxes. In fact, statistical uncertainties related to sky subtraction are usually negligible compared to calibration and systematic uncertainties. However, statistical uncertainties can be appreciable—tens of percent—for low-S/N sources (e.g., Dale et al. 2005). At 24 μm, this is clearly the case for A0620−00 and V404 Cyg, which are both affected by high-cirrus background, as is apparent from Figure 1.

3. RADIO/INFRARED/OPTICAL SPECTRA

We first compile the SEDs of the three systems by putting together the *Spitzer* data discussed above, plus optical and radio

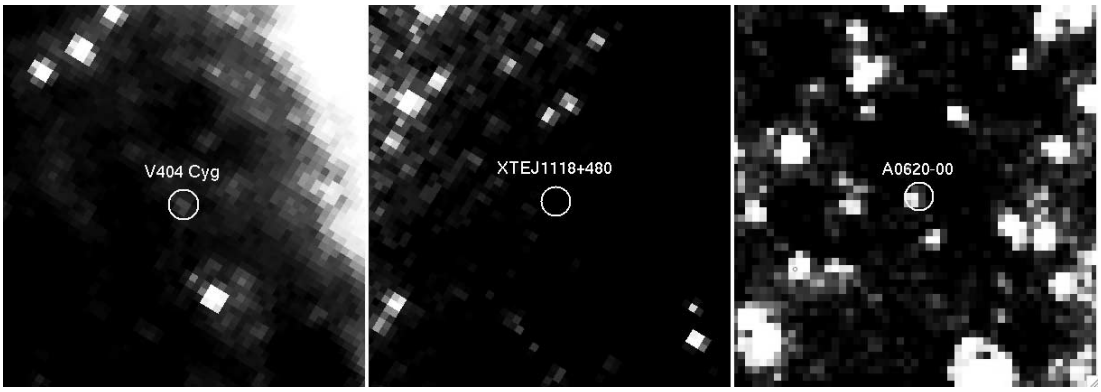

FIG. 1.—*Spitzer* MIPS 24 μm images of V404 Cyg, XTE J1118+480, and A0620−00. White circles (with 2″ radius) mark the positions of the radio counterparts from MERLIN and VLA observations for V404 Cyg (R. Spencer and M. Rupen, private communications); MERLIN observations for XTE J1118+480 (Fender et al. 2001); and VLA observations for A0620−00 (Gallo et al. 2006). The fields of view of V404 Cyg and A0620−00 are evidently affected by high background contaminations, resulting in high statistical uncertainties related to sky subtraction. For reference, 1 MIPS pixel corresponds to 1.2″ in size. North is at the top, and east is to the left in these images. [*See the electronic edition of the Journal for a color version of this figure*.]

data available in the literature. For A0620−00, we make use of new optical data, presented in § 3.3.1. Clearly, the nonstrict simultaneity of the observations, combined with the known variability of quiescent BHBs at all wavelengths (e.g., Hynes et al. 2003, 2004), should be kept in mind before drawing any definitive conclusion on the modeling. Figure 2 shows the broadband SEDs of V404 Cyg, XTE J1118+480, and A0620−00 while in the quiescent state, from radio to optical wavelengths.

We first focus on the IR/optical spectra. Unlike MM06, we do not compare the data against stellar atmosphere models: the smoothness of our SEDs does not demand a sophisticated model which can account for fine spectral features. Most importantly, we aim to quantify the relative goodness of the various models via proper χ^2 fitting, which would be meaningless if we were to apply stellar atmosphere codes to our sparse data points. Hence, for each object we first model the IR/optical spectrum with a single-temperature blackbody, using the best available estimates for the source distance, inclination, and effective temperature. The blackbody approximation is meant to mimic the contribution from the donor star. As shown by MM06, the contribution from the irradiated outer accretion disk is negligible for the parameter space relevant to these quiescent systems, at least in the IR band. The best-fitting blackbody curves are shown in the left panels of Figure 3, with the fitted parameters and reduced χ^2 given in Table 2. Evidently, the single-blackbody model provides a poor fit to the data: excess mid-IR emission, with respect to the Rayleigh-Jeans tail of the donor/disk, is detected in all three cases.

TABLE 1

Spitzer OBSERVATIONS OF QUIESCENT BLACK HOLE BINARIES

TARGET	METHOD	FLUX (μJy)		
		4.5 μm	8.0 μm	24.0 μm
V404 Cyg.....	Ap. photometry	3336	1820	414 ± 220
	PRF fitting	3220	1760	436 ± 220
XTE J1118+480.....	Ap. photometry	69	59	<50
	PRF fitting	69	58	<50
A0620−00.....	Ap. photometry	412	288	138 ± 65
	PRF fitting	380	305	121 ± 65

NOTES.—Un-dereddened values. Unless otherwise noted, flux errors are taken to be 10%, due to calibration systematic errors. For the extinction corrections, we used the following values. V404 Cyg: $A_V = 2.8$ (Shahbaz et al. 2003). XTE J1118+480: $A_V = 0.06$ (Gelino et al. 2006). A0620−00: $A_V = 1.2$ (Wu et al. 1976).

Fitting the data with two blackbodies (Fig. 3, *middle panels*) slightly improves the reduced χ^2 in all cases (Table 3). The temperatures and normalizations of these secondary blackbodies imply indeed larger physical sizes than the orbital separation, possibly supporting the circumbinary material interpretation (MM06). However, radio emission has been detected in two of these sources (V404 Cyg; Hjellming et al. 2000, and A0620−00; Gallo et al. 2006), and interpreted as partially self-absorbed synchrotron emission from a relativistic outflow. The flat/slightly inverted outflow spectrum must become optically thin at higher frequencies, possibly in the mid-IR (R06). We thus explore the possibility that the mid-IR excess might be, at least partly, due to nonthermal emission from a jet. This possibility has been ruled

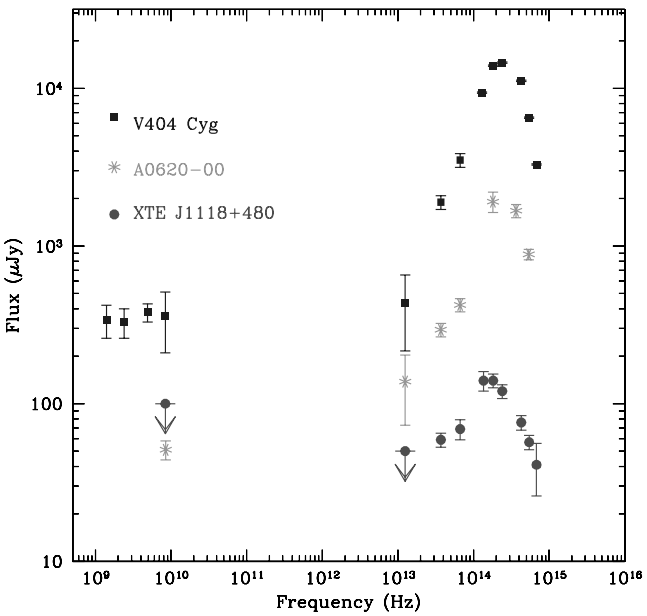

FIG. 2.— Composite radio/IR/optical spectra of quiescent black hole binaries. V404 Cyg: radio data from Gallo et al. (2005b), taken in 2002; IR data from this work, taken in 2004–2005; optical photometry from Casares et al. 1993, taken between 1990 and 1992. A0620−00: radio data from Gallo et al. (2006), acquired in 2005 August; IR and optical data from this work. The data span a period of 5 months, with nearly simultaneous radio/optical coverage. XTE J1118+480: radio upper limit from Mirabel et al. (2001); IR data from this work; optical photometry from Gelino et al. (2006). [*See the electronic edition of the Journal for a color version of this figure*.]

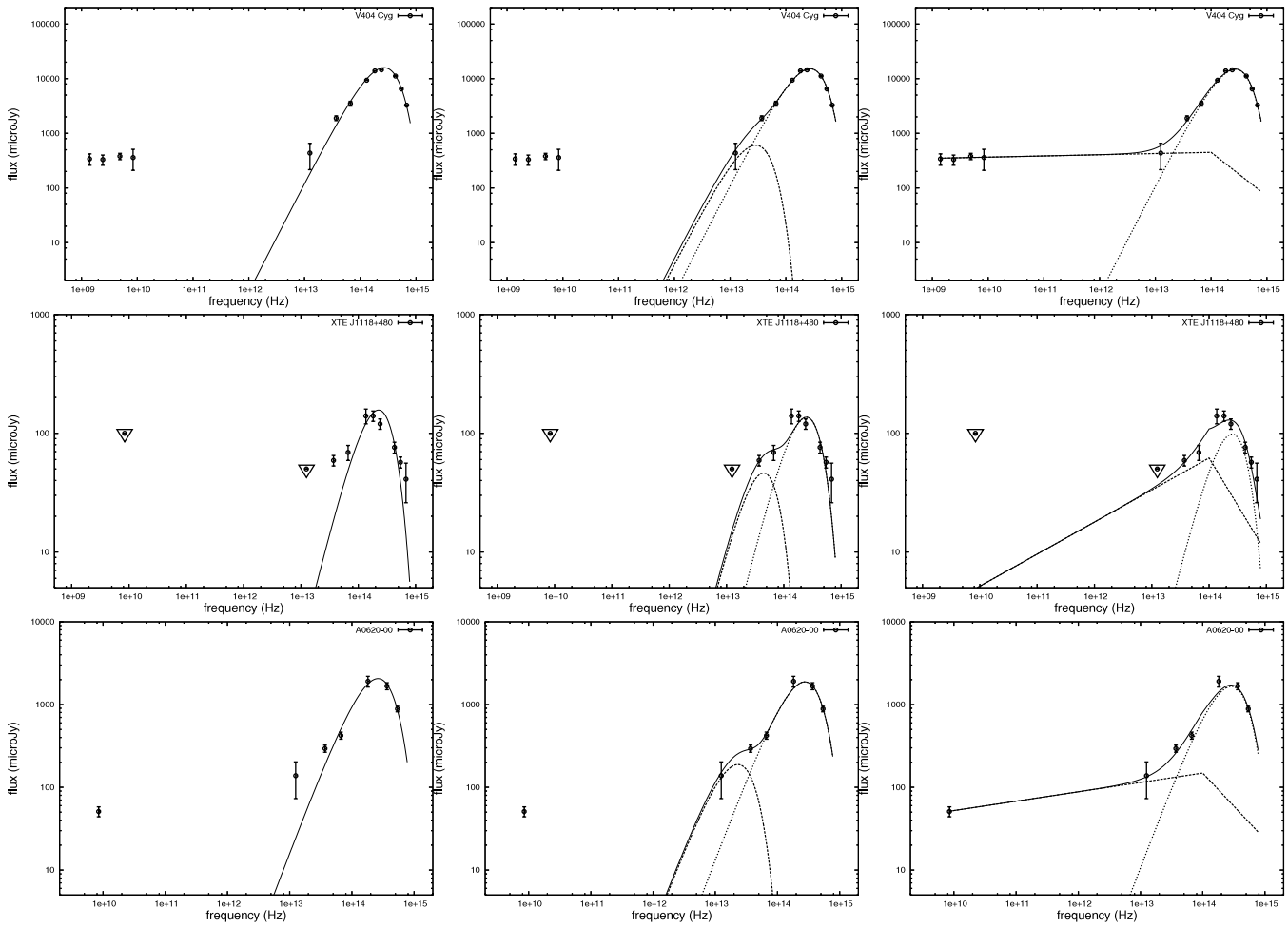

FIG. 3.—*From top to bottom*: V404 Cyg, XTE J1118+480, and A0620−00. Curves in the left panels show the fits to the IR/optical data with a single-blackbody curve (see Table 2 for the fitted parameters); curves in the middle panels are for a double-blackbody fit (Table 3); the right panels show the fit to the radio/IR/optical SEDs with a single-blackbody, plus a broken power law (Table 4).

out by MM06 on the basis of far too low fluxes/upper limits at 24 μm. However, our revised estimates for the 24 μm rms noise levels leave this possibility open.

We choose to fit the *radio*/IR/optical SEDs with a single blackbody plus a broken power law of the form:

$$F_\nu = F_{\nu_0} \times \begin{cases} (\nu/\nu_0)^{\alpha_1}, & \nu < \nu_b, \\ (\nu_b/\nu_0)^{\alpha_1-\alpha_2}(\nu/\nu_0)^{\alpha_2}, & \nu > \nu_b. \end{cases} \quad (1)$$

This is meant to account for a partially self-absorbed synchrotron spectrum with index $\alpha_1 = 0.0-0.5$ up to the break frequency ν_b, above which it becomes optically thin with index α_2. After running a grid of models with all six fitting parameters (blackbody temperature and normalization, plus the four broken power-law parameters) free to vary, we choose to fix the index of the optically thin portion to $\alpha_2 = -0.8$ [corresponding to a "canonical" electron distribution $N(E) \propto E^{-p}$ with power-law index $p = +2.6$, E being the electron energy; e.g., Fender 2006] and the position of the break to $\nu_b = 10^{14}$ Hz, in order to maximize the jet contribution to the mid-IR band. The results of the blackbody plus broken power-law fits are shown in the right panels of Figure 3, with the fitted parameters in Table 4. We discuss below the SED compilation and the results of the modeling on a case-by-case basis.

TABLE 2
SINGLE BLACKBODY FITS TO THE IR/OPTICAL SPECTRA

Target (1)	R/D (2)	$T_{\rm fit}$ (3)	$T_{\rm star}$ (4)	χ^2/dof (5)
V404 Cyg.....	5.4 ± 0.2	4533 ± 80	5500	10.3/7
XTE J1118+480.....	0.7 ± 0.1	3850 ± 113	4250	69.6/5
A0620−00.....	2.0 ± 0.1	4468 ± 104	4900	21.8/4

NOTES.—Col. (1): Source name. Col. (2): Fitted star radius over distance, R/D, times 10^{-11}. Col (3): Fitted star temperature, $T_{\rm fit}$, in K. Col. (4): Star temperatures as found in the literature, $T_{\rm star}$, in K (references for the star temperature, system inclination, and distance are the same as listed in the caption of Table 1 for the extinction values). Col. (5) Fitted χ^2 over degrees of freedom (dof).

3.1. *V404 Cyg* (*GS 2023+338*)

Casares et al. (1993) report on *B*-, *V*-, *R*-, *J*-, *H*-, and *K*-band photometry of V404 Cyg taken from 1991 July to August, 2 years after the end of the 1989 outburst that preceded the current quiescent regime (even though this system, because of its relatively high quiescent X-ray luminosity [$L_{\rm X}/L_{\rm Edd} \simeq 10^{-6.5}$], is often considered at the boundary between quiescence and the hard X-ray state). Several later works have established V404 Cyg to be variable by a factor of a few at IR-to-X-ray wavelengths (see, e.g., Hynes et al. 2004, Bradley et al. 2007 for the X-ray/optical variability; Zurita et al. 2004 and references therein for a study of the long term optical/IR variability). The origin of such variability is yet to be well understood, even though there is general

TABLE 3
Double Blackbody Fits to the IR/Optical Spectra

Target (1)	$(R/D)_1$ (2)	$T_{\rm fit,1}$ (3)	$(R/D)_2$ (4)	$T_{\rm fit,2}$ (5)	χ^2/dof (6)
V404 Cyg.....	5.09 ± 0.02	4623 ± 94	30 ± 18	489 ± 169	1.4/5
XTE J1118+480.....	0.55 ± 0.04	4234 ± 150	4 ± 1	754 ± 140	12.0/3
A0620−00.....	1.7 ± 0.1	4691 ± 149	23 ± 10	393 ± 83	2.0/2

Notes.—Col. (1): Source name. Cols. (2), (4): Fitted blackbody radius over distance $\times 10^{-11}$. Cols. (3), (5): Fitted blackbody temperature, in K. Col. (6): Reduced χ^2. Subscripts 1 and 2 indicate the first and second blackbody components.

agreement that it should take place somewhere in the accretion flow rather than in the hot gas stream/donor star (Shahbaz et al. 2003; Zurita et al. 2003; Hynes et al. 2003, 2004).

Over the past few years, V404 Cyg has been known as a relatively stable radio source, with an average flux density of $\sim$350 μJy, and a flat/slightly inverted spectrum at GHz frequencies (Hjellming et al. 2000; Gallo et al. 2005b), interpreted in terms of partially self-absorbed synchrotron radiation from outflowing plasma. The variable nature of this system, combined with the fact that the available data spread an interval of several years (the optical and *Spitzer* data were acquired more than 10 years apart), make it especially difficult to draw definite conclusions about the mid-IR emission detected with MIPS (on the other hand, R06 showed that the optical/IR luminosity of hard/quiescent state sources scales with the X-ray luminosity to the power 0.6, implying that the X-ray variability should be reduced to some extent in the IR).

The top panels of Figure 3 show the IR/optical spectrum of V404 Cyg as fitted with a single- and double-blackbody model (*left and middle panel, respectively*); clearly, the latter model provides a better fit to the IR/optical data, with $\chi^2/{\rm dof} = 10.3/7$ and $\chi^2/{\rm dof} = 1.4/5$, respectively. However, these components do not account for the radio emission. Because of the flat radio spectrum, the possibility cannot be ruled out that the excess emission at 24 μm might be due to the high-frequency portion of the well-established synchrotron-emitting outflow. The top right panel of Figure 3 shows a fit to the radio/IR/optical data with a single blackbody with $T \simeq 4600$ K, plus a broken power law, where the fitted index of the partially self-absorbed regime is $\alpha_1 = 0.02$. This two-component model provides as a good fit as the double-blackbody model ($\chi^2/{\rm dof} = 4.0/9$), and it also accounts for the radio emission.

This suggests that, in this system, synchrotron emission from a partially self-absorbed outflow is likely to be responsible for the observed mid-IR excess as much as thermal emission from circumbinary material. As an aside, if such excess were entirely due to circumbinary disk emission, this would imply that the jet break to the optically thin portion has to occur somewhere in the millimeter regime, i.e., at lower frequencies than predicted by R06. While the system SED could be comfortably reproduced by the sum of two blackbody components plus a broken power law, accommodating the circumbinary material and the jet contribution would require as many free parameters as data points.

3.2. *XTE J1118+480*

Gelino et al. (2006) present *B*-, *V*-, *R*-, *J*-, *H*-, and K_s-band photometry of XTE J1118+480 in quiescence. Due to its high Galactic latitude, XTE J1118+480 is a virtually unabsorbed source ($A_V = 0.06$), and yet it can be taken as an example of how tricky it can be to infer the properties and the geometry of the accretion flow based on modeling the SED. For instance, the high-quality simultaneous multiwavelength data acquired while in the hard state (at $L_{\rm X}/L_{\rm Edd} \simeq 10^{-3}$) have been successfully modeled in terms of an advection-dominated accretion flow (McClintock et al. 2003; Yuan et al. 2005), as well as by using a jet synchrotron model (Markoff et al. 2001). As shown in Figure 3 (*middle panels*), there is evidence for substantial excess emission at 8 μm with respect to the donor star tail. We notice that the single-blackbody model provides a very poor representation of the donor star spectrum; in this case, the actual stellar atmosphere model is certainly more appropriate (see MM06, Figure 2). However, as noted above, we are interested in constraining the nature of the excess mid-IR emission via proper χ^2 fitting; in this framework, our goal is to determine whether fitting the mid-IR excess with a broken power-law model provides a better or worse description of the data in a statistical sense, irrespective of how well the donor star thermal emission is modeled. The radio counterpart to XTE J1118+480 is undetected in quiescence, with an upper limit of 0.1 mJy at 8.5 GHz (Mirabel et al. 2001). Because of this shallow upper limit, the measured excess at 8 μm might still be interpreted as being due to a partially self-absorbed outflow that extends its power-law spectrum from the radio up to the IRAC regime. This is illustrated in the middle right panel of Figure 3, where a partially self-absorbed synchrotron-emitting outflow with $\alpha_1 = 0.27$, plus a $\sim$4300 K blackbody component, account for the system SED. The reduced χ^2 is improved with respect to the double-blackbody

TABLE 4
Blackbody and Broken Power-Law Fits to the Radio/IR/Optical Spectra

Target (1)	(R/D) (2)	$T_{\rm fit}$ (3)	F_{ν_0} (4)	α_1 (5)	χ^2/dof (6)
V404 Cyg.....	5.0 ± 0.2	4626 ± 94	448 ± 189	0.02 ± 0.04	4.0/9
XTE J1118+480.....	0.5 ± 0.1	4302 ± 211	62 ± 23	0.27 ± 0.39	6.2/3
A0620−00.....	1.54 ± 0.03	4897 ± 6	148 ± 1	0.113 ± 0.001	7.8/3

Notes.—Cols. (1)–(3): see Table 1. Col. (4): Fitted power-law normalization at $\nu_0 = 10^{14}$ Hz, in μJy (the broken power-law expression is given in eq. [1]; we fixed $\nu_b = 10^{14}$ Hz and $\alpha_2 = -0.8$). Col. (5): Fitted power-law index below ν_b. Col. (6): Reduced χ^2.

TABLE 5
A0620−00: SMARTS Observations

Band	UT start	mag[a]	Flux[b] (μJy)
V.....	2005 Aug 18, 09:28:15	17.75 ± 0.03	884 ± 68
I.....	2005 Aug 18, 09:19:31	16.04 ± 0.05	1673 ± 161
H.....	2005 Aug 18, 09:28:12	14.6 ± 0.1	1910 ± 283

[a] Un-dereddened values.
[b] Dereddened values (adopting $A_V = 1.2$), allowing for an extra 0.05 mag uncertainty due to systematic calibration errors.

model (χ^2/dof $= 12.0/3$ vs. 6.2/3 for the double-blackbody and blackbody plus broken power-law model, respectively). Within the blackbody plus power-law model, the fitted values for the blackbody temperature and normalization are consistent, within the errors, with the inferred values for the donor star (namely $\sim$4250 K and $\simeq$0.4 $R_\odot$; Gelino et al. 2006). The fitted radio spectral index is consistent with hard-state sources (Fender 2001), and predicts a GHz flux density lower than 5 μJy, which is practically undetectable with current radio facilities over reasonable integration times (the rms noise level for a 24 hr integration with the VLA is about 5 μJy at 8.5 GHz; however, planned upgrades, such as the eMERLIN and EVLA, will be able to probe such flux density levels in hours-long exposures).

3.3. *A0620−00* (*V616 Mon*)

3.3.1. *SMARTS Observations*

We construct the SED of A0620−00 by means of radio, IR, optical, and X-ray observations, all taken in 2005; the optical/near-IR data were acquired by the Small and Moderate Aperture Research Telescope System (SMARTS[9]) consortium, using the Cerro Tololo Inter-American Observatory 1.3 m, together with ANDICAM,[10] a dual-channel imager capable of obtaining optical and IR data simultaneously. A0620−00 was observed through *I*, *V*, and *H* filters on 2005 August 18, one day before the beginning of the (strictly simultaneous) Chandra/VLA observations (taken on 2005 August 19–20; Gallo et al. 2006), while the *Spitzer* data discussed above were acquired on 2005 March 06 (MIPS) and March 25 (IRAC).

SMARTS data were calibrated using data from previous nights and were processed and reduced using standard IRAF aperture photometry routines. The measured magnitudes were converted into fluxes using the SMARTS photometric zero-points; we used a color excess of $E(B-V) = 0.39 \pm 0.02$ (Wu et al. 1976), and corrected for extinction by again following the standard prescription for the frequency-variable absorption by Cardelli et al. (1989). The results are summarized in Table 5. Interestingly, all of the measured magnitudes are brighter than the maximum magnitude from the previously published quiescent light curves (see Table 1 in Gelino et al. 2001, which reports on optical and IR observations of A0620−00 between 1976 and 2001), and from 0.5–0.7 mag brighter than the mean magnitudes. However, given the observed trend of increasing brightness in this source over the past few years, it seems very unlikely that these results require a sudden flare. This, however, has to be kept in mind when inspecting the whole SED of A0620−00, in particular when comparing the 2005 March *Spitzer* observations with the optical and near-IR values given by Gelino et al. (2001).

[9] See http://www.astro.yale.edu/smarts.
[10] See http://www.astronomy.ohio-state.edu/ANDICAM.

3.3.2. *Broadband SED*

Significant excess emission with respect to the Rayleigh-Jeans portion of the donor's blackbody spectrum is detected at 8 and 24 μm. As shown in the middle-bottom panel of Figure 3, the sum of two blackbodies ($\sim$4700 + 390 K) provides a good fit to the IR/optical data (χ^2/dof $= 2.0/2$). The detection of a radio counterpart to A0620−00 strongly suggests that this quiescent system is powering a synchrotron-emitting outflow (Gallo et al. 2006). By analogy with hard state systems (Fender 2001), it is reasonable to assume that the partially self-absorbed portion of the jet has a flat spectrum. Such a spectrum would have to become optically thin at frequencies lower than 10^{13} Hz for it not to contribute to the mid-IR excess. Alternatively, the whole radio/IR/optical spectrum can be well fit by the sum of an $\sim$4900 K blackbody plus a broken power law, with a slightly inverted spectrum in the radio/IR regime with $\alpha_1 = 0.1$ (yielding χ^2/dof $= 7.8/3$).

4. ORIGIN OF THE MID-IR EXCESS: IMPLICATIONS FOR THE JET POWER

The *Spitzer* observations of the three quiescent BHBs discussed above show evidence for excess emission in the mid-IR band; while it may possible to reproduce the emission between $2–4 \times 10^{14}$ Hz with a blackbody whose temperature is consistent with the shown temperatures of the secondary stars, it would be difficult to explain the excess at 10^{13} Hz with any model for which the temperature is high enough to move 10^{13} Hz into the Rayleigh-Jeans portion of the blackbody spectrum. Thus, two main possibilities arise to account for the measured excess: thermal emission from cool (hundreds of K) circumbinary material, or synchrotron emission from outflowing plasma. The latter hypothesis was dismissed by MM06 on the basis of far too low 24 μm fluxes/upper limits. Our estimates for the statistical uncertainties on the 24 μm observations, however, reinstate this possibility.

Under the assumption that nonthermal synchrotron emission is at the origin of the measured IR excess, we can estimate the amount of power stored in the outflows. Integrating the partially self-absorbed jet spectra up to 10^{14} Hz, and assuming a (conservatively low) jet radiative efficiency of 5%, and no Doppler boosting (see Fender 2001), we obtain jet powers in the range $\sim 4 \times 10^{32}$ erg s^{-1} for A0620−00 and XTE J1118+480, the lower Eddington-ratio sources, up to $\sim 2 \times 10^{34}$ erg s^{-1} for V404 Cyg (see Table 6). Under these assumptions, the total jet power exceeds the measured X-ray luminosities (between 2 and 10 keV) in quiescence by a factor of at least 50. Assuming that the steep X-ray power laws observed in quiescent BHBs (with average photon index $\Gamma \simeq 2$; e.g., Corbel et al. 2006) extend up to $\sim$100 keV, where a spectral cutoff is observable in higher Eddington-ratio systems, the *bolometric* (0.1–100 keV) X-ray luminosities are likely to exceed the measured 2–10 keV luminosities by a factor of a few. Therefore, this regime of $L_{j,\rm tot} \gtrsim L_{\rm X}$ fits the definition of jet-dominated state put forward by Fender et al. (2003). The above estimates of $L_{j,\rm tot}$ are based on a conservative radiative efficiency for the synchrotron process of 5%; as such, they represent strict lower limits. Alternatively, we can estimate the total jet power by following the formalism by Heinz & Grimm (2005), in which the monochromatic radio core emission (L_r, in units of 10^{30} erg s^{-1}) of three well-studied radio galaxies was directly compared to the radio lobe emission, and combined with a self-similar jet model (Heinz & Sunyaev 2003) in order to calibrate the ratio of mechanical versus radiative power of partially self-absorbed jets. They proposed that the jet kinetic power of

TABLE 6
JET POWER

Target (1)	α_1 (2)	D (3)	$L_{j,\rm tot}$ (4)	$L_{j,\rm rad}/L_{\rm X}$ (5)
V404 Cyg	0.022	4	$>1.7\times10^{34}$	2.8
XTE J1118+480	0.270	1.8	$>3.7\times10^{32}$	5.4
A0620−00	0.113	1.2	$>4.5\times10^{32}$	3.8

NOTES.—Col. (1): Source name. Col (2): Fitted jet spectral index below $\nu_b = 10^{14}$ Hz. Col (3): Distance, in kpc. Col. (4): Total (kinetic + radiative) jet power, in erg s^{-1}. Col. (5): Ratio between the radiative jet power, integrated up to ν_b, and the quiescent X-ray luminosity $L_{\rm X}$, between 2–10 keV. $L_{j,\rm tot}$ is calculated assuming no Doppler boosting, and a (conservative) 5% radiative efficiency; as such, it represents a strict lower limit to the total jet power. Accordingly, $L_{j,\rm rad} = 0.05 \times L_{j,\rm tot}$ only accounts for the partially self-absorbed synchrotron emission from the jet. Quiescent X-ray luminosities for V404 Cyg are from Garcia et al. (2001), Kong et al. (2002), and Hynes et al. (2004); for XTE J1118+480 from McClintock et al. (2004); and for A0620−00 from Kong et al. (2002) and Gallo et al. (2006).

both supermassive and stellar size BHs can be estimated from the core radio luminosity as

$$L_{j,\rm tot} = 6.2\times10^{37} L_r^{1/(1.4-\alpha_r/3)} \mathcal{W}_{37.8}\ \rm erg\ s^{-1},$$

where α_r is the radio spectral index over the partially self-absorbed regime, and the parameter $\mathcal{W}_{37.8}$ carries the (quite large) uncertainty on the radio galaxy calibration. The normalization value by Heinz & Grimm is roughly in agreement with that estimated by Körding et al. (2006); here, for flat spectrum radio sources, the jet power (at the hard to soft state transition) is expressed as

$$L_{j,\rm tot} \lesssim 3.6\times10^{37} (f/0.75)(\eta/0.1) L_r^{(12/17)}\ \rm erg\ s^{-1},$$

where f is the fraction of outer mass accretion rate that is not expelled via winds/outflows, and η is the standard accretion efficiency. Either way, the inferred total jet power would exceed the *bolometric* X-ray luminosity by at least 4 orders of magnitude for the three quiescent BHBs under consideration. It is worth mentioning that, independently of normalization and efficiency factors, in all three cases the jet *synchrotron* luminosity, integrated up to 10^{14} Hz (that is, neglecting the optically thin portion), already exceeds the measured 2–10 keV luminosities by a factor of a few (Table 6, right column).

In contrast, if thermal emission from circumbinary disk material is entirely responsible for the measured mid-IR excess, this would imply that the jet spectrum breaks at much lower frequencies, perhaps in the far-IR/millimeter regime, lowering the above estimates by a factor of 10 at least. A final test to assess the origin of the measured excess could be a variability study in the mid-IR, possibly coordinated with the radio.

5. A MAXIMALLY JET-DOMINATED MODEL FOR THE QUIESCENT STATE

Ultimately, as discussed by McClintock et al. (2003), while there is general agreement that the X-ray emission in quiescent BHBs comes from high-energy electrons near the BH, there is disagreement regarding (1) the attribution of the emission to outflowing versus inflowing electrons and (2) the modeling of the electron distribution as thermal versus nonthermal (or hybrid). The SEDs of quiescent BHBs, as well as low-luminosity AGNs, are often examined in the context of the advection-dominated accretion flow model (Narayan & Yi 1994), whereby the low X-ray luminosities are due to a highly reduced radiative efficiency, and most of the liberated accretion power disappears into the horizon. Alternatively, building on the work by Falcke & Biermann (1996) on AGN jets, a jet model has been proposed for hard-state BHBs. The model is based on four assumptions: (1) that the total power in the jets scales with the total accretion power at the innermost part of the accretion disk, $\dot{m}c^2$, (2) that the jets are freely expanding and are only weakly accelerated via their own internal pressure gradients only, (3) that the jets contain cold protons which carry most of the kinetic energy, while leptons dominate the radiation, and (4) that some fraction of the initially quasi-thermal particles are accelerated into power-law tails. Markoff et al. (2001) argued that jet synchrotron emission could account for the broad continuum features of the simultaneous radio through X-ray observations of XTE J1118+480 while in the hard state. This same model was also able to explain the broad spectral features of 13 quasi-simultaneous radio/X-ray observations of GX 339−4, and to reproduce the observed nonlinear radio/X-ray correlation in this system (Corbel et al. 2003) by varying the amount of power channeled in the jet (Markoff et al. 2003). Based on the required reflection signatures, a new model was developed (Markoff et al. 2005, hereafter MNW05) which could reproduce the simultaneous radio/X-ray data of hard-state systems (GX 339−4 and Cygnus X-1) via radiation from a compact, mildly relativistic jet, combined with a truncated thermal disk. In particular, the X-ray emission can be interpreted as a combination of optically thin synchrotron emission predominantly from an acceleration region ~10–100 gravitational radii along the jets, plus external (thermal disk photons) and synchrotron self-Compton emission from the base of the jets, in a region associated with a magnetic compact corona. The radio through the soft X-rays are dominated by synchrotron emission, while the hard X-rays are mostly Comptonization, with weak reflection. This *maximally jet-dominated model* was intended to explore the possibility that the hot electron corona and jet base may be intimately related, or, in the extreme case, synonymous (we refer the reader to MNW05 for a fuller description). This model has been tested extensively on simultaneous radio and X-ray data, and for a number of hard-state BHBs. The mid-IR portion of the spectrum is clearly crucial in order to put constraints on the optically thick-to-thin jet breaks, as demonstrated by the *Spitzer* observations of the neutron star X-ray binary 4U 0614+091 (Migliari et al. 2006) and the BHB GRO 1655−40 (Migliari et al. 2007).

In the following, we attempt to fit the radio through X-ray SED of A0620−00 in quiescence via the maximally jet-dominated model, where full details can be found in the Appendix of MNW05. The choice of A0620−00 (over, e.g., V404 Cyg, for which the radio spectrum is well constrained) is motivated by the fact that, with the exception of the *Spitzer* data, the observations were acquired nearly simultaneously (the VLA and *Chandra* observations were strictly simultaneous, while the SMARTS observations were taken only 1 day earlier). As a comparison, the broadband SED of V404 Cyg is built on data sets that were taken over a span of 10 years. In addition, A0620−00 has been in quiescence for over 30 years, and is considered to be a stable and moderately variable system, while V404 Cyg is known to vary in flux by a factor of a few within hours (e.g., Hynes et al. 2003).

5.1. *Application to A0620−00*

The fitting was performed with the Interactive Spectral Interpretation System (ISIS; Houck & De Nicola 2000). As outlined in MNW05, the fitting is initiated outside ISIS in order to avoid local minima, using unfolded data that yield a set of starting parameters for which the reduced χ^2 is lower than 2. We decided to fix several parameters which previously have been allowed to vary, firstly because the results of fitting the model to several hard-state sources suggest that there may be canonical values, and secondly because of the low count rates. In spite of the

large luminosity difference between A0620−00 ($L_X/L_{Edd} \simeq 10^{-8}$) and other sources whose hard-state spectra were successfully fitted by the jet model, such as XTE J1118+480 (Markoff et al. 2001), GX 339−4, and Cygnus X−1 (both Markoff et al. 2005), simultaneous VLA and *Chandra* observations of A0620−00 in quiescence have shown that the nonlinear radio/X-ray correlation for hard-state BHBs appears unbroken all the way down to $10^{-8}L_{Edd}$, which argues for no substantial difference between the hard and quiescent states (Gallo et al. 2006; but see Xue & Cui 2007 and Gallo 2007). On the other hand, recent high-statistics X-ray observations of hard-state BHBs seem to show that a geometrically thin disk is present and already extends close to the innermost stable orbit at $10^{-3}L_{Edd}$ (Miller et al. 2006b, 2006a; Rykoff et al. 2007). As such a solution would be very difficult to maintain at $10^{-8}L_{Edd}$, these authors conclude that a major transition has to take place at intermediate luminosities. Consequently, in light of the large degree of uncertainty regarding the nature and geometry of the accretion flow in quiescence, this must be considered as an exploratory study.

The model is most sensitive to the fitted parameter N_j, which acts as a normalization, although it is not strictly equivalent to the total power in the jets (see discussion in MNW05). It dictates the power initially divided between the particles and the magnetic field at the base of the jet, and is expressed in terms of a fraction of L_{Edd}. Once N_j is specified and conservation is assumed, the macroscopic physical parameters along the jet are determined assuming that the jet power is roughly shared between the internal and external pressures. The radiating particles enter the base of the jet where the bulk velocities are lowest, with a quasi-thermal distribution. Starting at location z_{acc} in the jets, a free parameter, 85% of the particles are accelerated into a power law with index p, also a fitted parameter. The maximum energy of the accelerated leptons is calculated by setting the acceleration rate to the local cooling rates from synchrotron and inverse Compton radiation at z_{acc}. If the acceleration process is diffusive Fermi acceleration, the acceleration rate depends on the factor $f = (u_{acc}/c)^2/f_{sc}$, where u_{acc} is the shock speed relative to the bulk plasma flow, and f_{sc} is the ratio of the scattering mean free path to the gyro-radius. Because neither plasma parameter is known, we fit for their combined contribution via f, which thus reflects the *efficiency of acceleration*. The particles in the jet radiatively cool via adiabatic expansion, the synchrotron process, and inverse Compton up-scattering; however, adiabatic expansion is assumed to dominate the observed effects of cooling. A weak thermal accretion disk is assumed to be present, with an inner disk temperature fixed (somewhat arbitrarily) at $T = 10^6$ K, or ~90 eV (inner disk temperatures between 50 and 200 keV are typically obtained for higher Eddington-ratio sources). This component is also included in Figure 4, and its photons are considered for local inverse Compton up-scattering. However, they are negligible compared to the photons produced by synchrotron radiation. The other main model parameters are the electron temperature T_e and the equipartition parameter between the magnetic field and the radiating (lepton) particle energy densities, k. A blackbody with temperature 4900 K, consistent with the companion star (Casares et al. 1993), is added to the model to account for the optical emission. An additional blackbody component has been also added to the fit, with normalization free to vary, in order to account for a possible contribution from the outer disk. These photons are also included in the Comptonization. The ratio of the "nozzle" (i.e., the pre-acceleration region) length to its radius has been fixed at 1.5, based on results in MNW05. The inclination angle between the jet axis and line of sight i has been fixed at 43°, the mass at 9.7 $M_\odot$, and the distance at 1.2 kpc, according to the recent results by Froning et al. (2007). We wish to stress that adopting the system parameters inferred by Gelino et al. (2001), i.e., 11 $M_\odot$ for the BH mass and $i = 40.75°$, does not result in a substantial change of the fitted parameters. Starting with parameter values similar to those found in other hard-state BHBs, we have obtained a reasonable fit to the data, with $\chi^2/\mathrm{dof} = 14.3/11$. The best fit model is shown in Figure 4, with parameters and 90% confidence error bars given in Table 7.

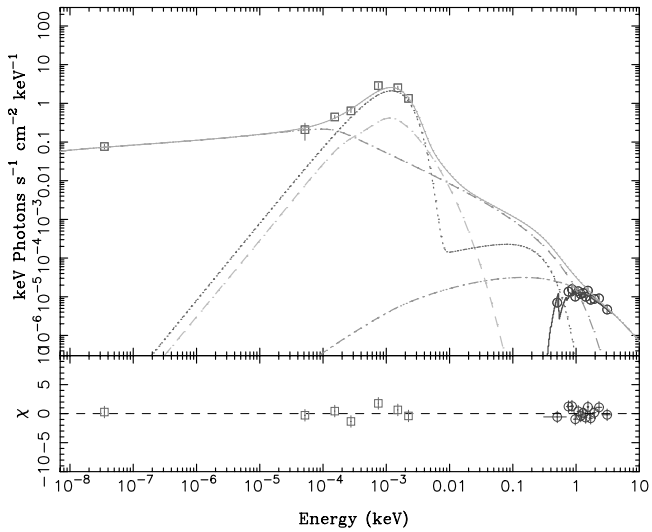

FIG. 4.—Jet model fit to broadband A0620−00 data with residuals. The symbols represent the data, while the solid red line is the model fit in detector space. Other indicated components are not convolved with the detector matrices, nor do they include absorption; they serve only to illustrate how the various emission mechanisms and regions contribute to the continuum. *Solid gray line*: total spectrum. *Dot-long-dashed yellow line*: pre-acceleration inner jet synchrotron emission; *dotted green line*: postacceleration outer jet synchrotron; *triple dot-dashed orange line*: Compton emission from the inner jet, including external disk photons as well as synchrotron self-Compton; *double-dot-dashed magenta line*: thermal multicolor-blackbody disk model plus single blackbody representing the star. See Table 7 for the fitted parameters. [*See the electronic edition of the Journal for a color version of this figure*.]

5.2. *Comparison to Hard State Sources*

Most of the free parameters have landed in ranges which we are starting to recognize as typical based on higher luminosity sources such as Cyg X-1 and GX 339-4 (MNW05), GRO J1655−40 (Migliari et al. 2007) and the low-luminosity AGN M81* (S. Markoff et al., in preparation). Interestingly, the two main differences appear to be related to the acceleration and equipartition. In higher luminosity sources we have found ratios of magnetic energy density to the energy densities in radiating particles on the order of ~1−5, while here our best-fit value actually favors a slight domination of the particle energy over the magnetic field ($0.1 < k < 0.2$). The low error bar was limited by the value 0.1, and thus does not represent a complete exploration of the parameter space. Nevertheless, exact equipartition appears to be ruled out, which points toward a change in energy distribution.

What is quite different compared to higher luminosity sources, however, is the required high-energy cutoff in the optically thin synchrotron component, and thus in the accelerated electron population. This is determined by comparing the acceleration parameter f to the local cooling rates. We find f to be around 2 orders of magnitude lower for A0620−00 than in higher luminosity sources. Interestingly, the only other black hole with similarly weak accretion that we can currently study is Sgr A*, the Galactic center supermassive BH. In fact, the jet model was first developed in simplified form by Falcke & Markoff (2000), with the aim of determining whether the same kind of model that could explain

TABLE 7
JET MODEL FOR A0620−00

Parameter	Value
$N_{\rm H}$[a]	$3.6^{+0.7}_{-1.1}$
N_j[b]	$14.6^{+0.4}_{-7.3}$
r_0[c]	$3.9^{+2.2}_{-0.1}$
$z_{\rm acc}$[d]	25^{+272}_{-2}
T_e[e]	$2.57^{+0.29}_{-0.01}$
p[f]	$2.5^{+0.1}_{-0.3}$
f[g]	$5.1^{+1.0}_{-1.5}$
k[h]	$0.1^{+0.1}_{-0.0}$
$\rm BB_{norm}$[i]	$0.5^{+0.2}_{-0.1}$

[a] Fitted hydrogen equivalent column density, in 10^{22} cm^{-2}.
[b] Model internal normalization, in units of $10^{-4}L_{\rm Edd}$, which dictates the power shared by the particles and the magnetic field at the base.
[c] Jet base (or "nozzle") radius, in units of gravitational radii $r_g = GM_{\rm BH}/c^2$.
[d] Acceleration region, $z_{\rm acc}$, in r_g, which sets the location along the jet at which (a fraction of) the particles start being accelerated.
[e] Temperature of the relativistic quasi-Maxwellian distribution with which the leptons enter the jet, in 10^{10} K.
[f] Power-law index of the accelerated electron distribution p, where $N(E) \propto E^{-p}$.
[g] Acceleration parameter f, in units of 10^{-6}, which sets the balance between particle acceleration and radiative plus adiabatic cooling, such that the quasi-thermal particles are energized into a power-law tail.
[h] Equipartition parameter, $k = (u_B/u_{\rm rad})$, i.e., the ratio between the energy density in radiating leptons and the magnetic field energy density.
[i] Internal disk blackbody normalization, in 10^{30} erg s^{-1}.
We fixed the BH mass, distance, and inclination of A0620−00 to 9.7 $M_\odot$, 1.2 kpc, and 43° (Froning et al. 2007), yielding $\chi^2_{\rm red} = 1.3$. Similar parameters, within the errors, are obtained adopting a mass of 11 $M_\odot$ and an inclination of 40.75° (Gelino et al. 2001). Error bars are given at the 90% confidence level.

the inverted radio spectrum of Sgr A* could also account for the newly discovered X-ray emission (Baganoff et al. 2000). They concluded that the SED of Sgr A* does not require a power law of optically thin synchrotron emission after the break from its flat/inverted radio spectrum. Therefore, if the radiating particles have a power-law distribution, it must be so steep that it is indistinguishable from a Maxwellian in the optically thin regime, i.e., they must be only weakly accelerated.[11] Here we have shown that something similar, albeit less extreme, is occurring in the quiescent BHB A0620−00; both scenarios imply that acceleration in the jets is absent or very inefficient at 10^{-9}–$10^{-8}L_{\rm Edd}$.

6. SUMMARY

We compile the radio/IR/optical spectra of three quiescent BHBs: V404 Cyg, XTE J1118+480, and A0620−00, for which we also present new optical SMARTS observations. Re-analysis of the archival *Spitzer* MIPS data for these systems yields systematically higher values for the statistical uncertainties related to sky subtraction with respect to the standard ∼10% value typically quoted for bright pointlike sources. While our revised values for the 24 μm fluxes are still consistent with those given by MM06 at the 3 σ level, they allow for a different interpretation of the measured mid-IR excess with respect to the tail of the donor star thermal component. We suggest that nonthermal emission from a jet could be responsible for a significant fraction (or all) of the measured excess mid-IR emission. While this possibly may not rule out the presence of circumbinary material, we argue that the radio/IR/optical spectra of the three BHBs under consideration do not require, in a statistical sense, the presence of an additional thermal component. A variability study could definitively address the question of the origin of the mid-IR excess, as, contrary to nonthermal jet emission, circumbinary disk emission is expected to be steady.

If nonthermal emission from a partially self-absorbed outflow is indeed responsible for the measured mid-IR excess, then the synchrotron luminosity of the jet exceeds the measured 2–10 keV luminosity by a factor of a few in all three systems, even when the optically thin radiation from the base is excluded. In turn, the jet mechanical power in quiescence is greater than the bolometric (0.1–100 keV) X-ray luminosity by several ($\gtrsim$4) orders of magnitude.

We proceed by focusing on A0620−00, the lowest Eddington-ratio BHB with a known radio counterpart, and construct its quiescent SED by adding VLA, *Spitzer*, SMARTS, and *Chandra* data. In spite of the nonsimultaneity of the *Spitzer* observations with the radio/optical/X-ray observations (which were taken over a 2 day period), we fit its broadband SED of A0620−00 with a maximally jet-dominated model (MNW05). This is the first time that such a complex model has been applied in the context of quiescent BHBs, and with the strong constraints on the jet break frequency cut-off provided by the *Spitzer* data in the mid-IR regime. In terms of best-fitting parameters, the major difference with respect to the higher luminosity sources for which this model has been successfully tested is in the value of the acceleration parameter f as compared to the local cooling rates, which turns out to be 2 orders of magnitude lower for A0620−00. This weak acceleration scenario is reminiscent of the Galactic center supermassive BH Sgr A*. Within the jet model working hypothesis, both SEDs are in fact consistent with the hard X-ray emission stemming primarily from inverse Compton processes in a corona/jet base dominated by quasi-thermal particles.

[11] In this framework, radically different particle distributions, such as power laws and Maxwellians, may result in similar fits, as long as the characteristic particle energy (minimum and peak energy for the power law and the Maxwellian, respectively) is similar. See MNW05, Appendix.

E. G. is funded by NASA through *Chandra* Postdoctoral Fellowship grant number PF5-60037, issued by the *Chandra* X-Ray Center, which is operated by the Smithsonian Astrophysical Observatory for NASA under contract NAS8-03060. J. A. T. acknowledges partial support from *Spitzer* contract number 1278068. C. D. B. is funded by NSF grant AST-0407063. S. B. acknowledges support by the Ing. Aldo Gini Foundation. We are grateful to Mike Nowak for providing us with the analysis scripts for ISIS.

REFERENCES

Baganoff, F., et al. 2000, BAAS, 32, 1389
Blandford, R., & Begelman, C. 1999, MNRAS, 303, L1
Bradley, C., Hynes, R., Kong, A., Haswell, C., Casares, J., & Gallo, E. 2007, ApJ, 667, 427
Cardelli, J., Clayton, G., & Mathis, J. 1989, ApJ, 345, 245
Casares, J., Charles, P. A., Naylor, T., & Pavlekno, E. P. 1993, MNRAS, 265, 834
Corbel, S., & Fender, R. 2002, ApJ, 573, L35
Corbel, S., Nowak, M., Fender, R. P., Tzioumis, A. K., & Markoff, S. 2003, A&A, 400, 1007

Corbel, S., Tomsick, J., & Kaaret, P. 2006, ApJ, 636, 971
Dale, D., et al. 2005, ApJ, 633, 857
Falcke, H., & Biermann, P. L. 1996, A&A, 308, 321
Falcke, H., & Markoff, S. 2000, A&A, 362, 113
Fazio, G., et al. 2004, ApJS, 154, 10
Fender, R. P. 2001, MNRAS, 322, 31
———. 2006, in Compact Stellar X-Ray Sources, ed. W. H. G. Lewin & M. van der Klis (Cambridge: Cambridge Univ. Press), 381
Fender, R. P., Gallo, E., & Jonker, P. G. 2003, MNRAS, 343, L99
Fender, R. P., et al. 2001, MNRAS, 322, L23
Froning, C., Robinson, E., & Bitner, M. 2007, ApJ, 663, 1215
Gallo, E. 2007, in AIP Conf. Proc. 924, The Multicolored Landscape of Compact Objects and their Explosive Origins, ed. L. A. Antonelli & L. Burderi (New York: AIP), 715
Gallo, E., Fender, R. P., & Hynes, R. I. 2005b, MNRAS, 356, 1017
Gallo, E., Fender, R. P., Kaiser, C., Russell, D., Morganti, R., Oosterloo, T., & Heinz, S. 2005a, Nature, 436, 819
Gallo, E., et al. 2006, MNRAS, 370, 1351
Garcia M. R., et al. 2001, ApJ, 553, L47
Gelino, D. M., Balman, S., Kiziloglu Ü., Yilmaz, A., Kalemci, E., & Tomsick, J. 2006, ApJ, 642, 438
Gelino, D. M., Harrison, T. E., & Orosz, J. E. 2001, AJ, 122, 2668
Heinz, S., & Grimm, H.-J. 2005, ApJ, 633, 384
Heinz, S., & Sunyaev, R. 2003, MNRAS, 343, L59
Hjellming, P. M., Rupen, M. P., Mioduszewski, A. J., & Narayan, R. 2000, ATel, 54, 1
Homan, J., & Belloni, T. 2005, Ap&SS, 300, 107
Homan, J., Buxton, M., Markoff, S., Bailyn, C., Nespoli, E., & Belloni, T. 2005, ApJ, 624, 295
Houck, J., & Denicola, L. 2000, in ASP Conf. Ser. 216, Astronomical Data Analysis Software and Systems IX, ed. N. Manset, C. Veillet, & D. Crabtree (San Francisco: ASP), 591
Hynes, R. I., et al. 2003, MNRAS, 345, 292
———. 2004, ApJ, 611, L125
Hynes, R. I., et al. 2006, ApJ, 651, 401
Kong, A. K. H., McClintock, J. E., Garcia, M. R., Murray, S. S., Barret, D. 2002, ApJ, 2002, 570, 277
Körding, E., Fender, R., & Migliari, S. 2006, MNRAS, 369, 1451
Makovoz, D., & Marleau, F. 2005, PASP, 117, 1113
Markoff, S., Falcke, H., & Fender, R. 2001, A&A, 372, L25
Markoff, S., Nowak, M. A., Corbel, S., Fender, R., & Falcke, H. 2003, A&A, 397, 645
Markoff, S., Nowak, M. A., & Wilms, J. 2005, ApJ, 635, 1203 (MNW05)
McClintock, J. E., Narayan, R., Rybicki, G. B. 2004, ApJ, 615, 402
McClintock, J. E., & Remillard, R. A. 2006, in Compact Stellar X-Ray Sources, ed. W. H. G. Lewin & M. van der Klis (Cambridge: Cambridge Univ. Press), 157
McClintock, J. E., et al. 2003, ApJ, 593, 435
Migliari, S., Tomsick, J., Maccarone, T., Gallo, E., Fender, R., Nelemans, G., & Russell, D. 2006, ApJ, 643, L41
Migliari, S. et al. 2007, ApJ, in press (arXiv:0707.4500)
Miller, J., Homan, J., & Miniutti, G. 2006a, ApJ, 652, L113
Miller, J., Homan, J., Steeghs, D., Rupen, M., Hunstead, R. W., Wijnands, R., Charles, P. A., & Fabian, A. C. 2006b, ApJ, 653, 525
Mirabel, I. F., Dhawan, V., Mignani, R., Rodrigues, I., & Giglielmetti, F. 2001, Nature, 413, 139
Muno, M., & Mauerhan, J. 2006, ApJ, 648, L135 (MM06)
Narayan, R., & Yi I. 1994, ApJ, 428, L13
Nowak, M. A., Wilms, J., Heinz, S., Pooley, G., Pottschmidt, K., & Corbel, S. 2005, ApJ, 626, 1006
Rieke, G., et al. 2004, ApJS, 154, 25
Russell, D., Fender, R., Gallo, E., & Kaiser, C. 2007, MNRAS, 376, 1341
Russell, D., Fender, R., Hynes, R., Brocksopp, C., Homan, J., Jonker, P., & Buxton, M. 2006, MNRAS, 371, 1334 (R06)
Rykoff, E., Miller, J., Steeghs, D., & Torres, M. 2007, ApJ, 666, 1129
Shahbaz, T., Dhillon, V. S., Marsh, T. R., Zurita, C., Haswell, C. A., Charles, P. A., Hynes, R. I., & Casares, J. 2003, MNRAS, 346, 1116
Taam, R., & Spruit, H. 2001, ApJ, 561, 329
Wang, Z., Chakrabarty, D., & Kaplan, D. 2006, Nature, 440, 772
Wu C.-C., Aalders, J., van Duinen, R., Kester, D., & Wesselius, P. 1976, A&A, 50, 445
Xue, Y., & Cui, W. 2007, A&A, 466, 1053
Yuan, F., Cui, W., & Narayan, R. 2005, ApJ, 620, 905
Zurita, C., Casares, J., Hynes, R., Shahbaz, T., Charles, P., & Pavlenko, E. 2004, MNRAS, 352, 877
Zurita, C., Casares, J., & Shahbaz, T. 2003, ApJ, 582, 369